SIMULTANEOUS COCRYSTALLIZATION AND MICRONIZATION OF PARACETAMOL-DIPICOLINIC ACID COCRYSTAL BY SUPERCRITICAL ANTISOLVENT (SAS)

STEVANUS HIENDRAWAN[a,b], BAMBANG VERIANSYAH[a], EDWARD WIDJOJOKUSUMO[a], SUNDANI NURONO SOEWANDHI[b], SALEH WIKARSA[b], RAYMOND R. TJANDRAWINATA[a*]

[a]Dexa Laboratories of Biomolecular Sciences, Cikarang 17550, West Java, Indonesia, [b]School of Pharmacy, Bandung Institute of Technology, Bandung 40132, West Java, Indonesia
Email: raymond@dexa-medica.com

ABSTRACT

Objective: This present study aims to produce cocrystal of paracetamol (PCA)-dipicolinic acid (DPA) using supercritical antisolvent (SAS) cocrystallization process in order to improve tabletability profile of PCA.

Methods: The PCA-DPA cocrystal prepared by SAS cocrystallization were compared to those produced using a traditional solvent evaporation. The cocrystals produced were characterized using Powder X-Ray Diffraction (PXRD), Differential Scanning Calorimetry (DSC), Thermogravimetric Analysis (TGA), Polarized Light Microscopy (PLM), Fourier Transform Infrared (FTIR) spectroscopy, particle size analysis, Scanning Electron Microscopy (SEM) and High Performance Liquid Chromatography (HPLC). Analysis of flowability, drug content, solubility, dissolution, stability and powder compaction were performed to evaluate the cocrystals.

Results: Cocrystal particles with mean diameter of 4.18 μm were produced from SAS process, smaller than those produced by traditional solvent evaporation method (mean diameter of 64.93 μm). The PCA-DPA cocrystal from SAS process showed an enhanced dissolution rate by 2.45 times compared to PCA, higher than cocrystal from traditional solvent evaporation (enhanced dissolution rate by 1.72 times compared to PCA). Tabletability study revealed superior tableting performance of both cocrystals compared to PCA.

Conclusion: This study showed the utility of PCA-DPA cocrystal to improve mechanical properties of PCA while also demonstrating that simultaneous micronization and cocrystallization process can be obtained using SAS process.

Keywords: Paracetamol, Dipicolinic acid, Cocrystal, Supercritical antisolvent, Tabletability, Micronization.

INTRODUCTION

During the past few years, interest in cocrystals research has increased significantly in several areas, including in pharmaceutical sector. Cocrystallization, one of the emerging crystal engineering techniques is a potential means for improving water solubility [1], which is a well-known obstacle in the drug development process. Apart from potential improvement in the solubility aspect, pharmaceutical cocrystals were also frequently used to enhance other essential physicochemical properties of the API such as chemical stability [2], hygroscopicity [3], dissolution rate [4], mechanical properties [5] and bioavailability [6] without interfering the pharmacological activity of the API. In addition, cocrystal formation also provides the opportunities for pharmaceutical industry to create the intellectual property and new patents of API for extending their life cycle [7]. A cocrystal can be defined as crystalline complexes consisting of multiple neutral components which are solid under ambient conditions. The components in a cocrystal exist in a definite stoichiometric ratio, which interact together in the crystal lattice through noncovalent interactions such as hydrogen bonds, π-π stacking and van der Waals interactions [8].

Pharmaceutical cocrystals have been produced using several methods such as mechanochemical (eg. neat and solvent drop or liquid-assisted grinding) [9-10] or by solution crystallization approaches (eg. solvent evaporation techniques, slurry techniques, cooling, anti-solvent addition and reaction crystallization methods) [11-13]. Other cocrystal screening methods such as using thermal microscopy, hot stage microscopy (Kofler technique) [14] and Differential Scanning Calorimetry (DSC) [15] have also been reported. However, all of these technologies possess several problems that should be considered in cocrystal scaling up and production scale. Recently, several attempts have been conducted to produce cocrystals using several processes that were suitable for

production scaling up, for example preparation of ibuprofen-nicotinamide cocrystal has been performed using hot melt extrusion [16]. However, hot melt extrusion process confers the risk of thermal degradation of the components due to high temperature used. Alhalaweh and Velaga [17] also conducted spray drying process to obtain cocrystals. This process has been successful in obtaining pure cocrystals from solutions under incongruent conditions which cannot be obtained from slow evaporation process. However, this method also shows its limitation that it produced amorphous product due to its rapid solidification during the process. In addition to several methods described above, a new approach using supercritical fluid (SCF) technology for Cocrystallization process has also been conducted successfully. Carbon dioxide (CO_2) at supercritical conditions is mainly used due to its relatively low critical temperature (31.1°C) and pressure (73.8 bar), nontoxic, nonflammable and inexpensive [18].

During the past years, the application of SCF especially supercritical CO_2 in the pharmaceutical particle design field has been widely studied. Several different processes based on dense CO_2 precipitation techniques and their modifications have been investigated such as rapid expansion of supercritical solutions (RESS), particles from gas-saturated solutions (PGSS), supercritical anti solvent (SAS), solution enhanced dispersion by supercritical fluids (SEDS), depressurization of an expanded liquid organic solvent (DELOS), and supercritical assisted atomization (SAA) [19]. Recent reports [20-26] presented feasibility studies for the production of pharmaceutical cocrystals using SCF techniques. Padrela *et al.* [20] have shown that indomethacin-saccharin cocrystal was produced in different morphologies and sizes either by SAS or supercritical enhanced atomization (SEA) technique. The same author also used SEA technique to screen various cocrystals of several APIs [21-22]. Batch gas anti-solvent (GAS) was also used for

the formation of itraconazole-succinic acid, itraconazole-l-malic acid cocrystals and also for naproxen-nicotinamide cocrystal [23-25]. RESS process has also been used to produce ibuprofen-nicotinamide cocrystal [26].

SAS technique is a single step process for Cocrystallization and micronization simultaneously. This process is suitable for compounds that have low solubility in SCF. In this process, a solution of an organic solvent is pumped through a nozzle into a chamber simultaneously with a SCF, which act as anti-solvent. The particles are generated due to the supersaturation of the solute within the solution droplet [27]. In this study, SAS process was used to produce pharmaceutical cocrystals between paracetamol (PCA) as the drug and dipicolinic acid (DPA) as the coformer. The resulting cocrystal was analyzed and compared with cocrystal from traditional solvent evaporation process. The SAS process previously showed its ability to produce submicron size of cocrystals [20]. In addition, PCA micronization using SAS has already been studied by several researchers [27-29].

PCA is a widely used analgesic and antipyretic drug that is commonly used for relieving fever, headaches and other minor aches and pains [30]. PCA is one of the most studied API for its solid form modification, i. e Cocrystallization and salt formation. From a crystal engineering viewpoint, PCA is a good API model for cocrystal design. As shown in fig. 1, PCA contains several functional groups, i. e amide and hydroxyl groups, which can act as donor and acceptor in hydrogen-bonding [31]. DPA (fig. 1) contains two carboxylic acid groups and one pyridine group that can act as a hydrogen bond donor and acceptor. Cocrystallization experiment of PCA and coformer 2,4-pyridinedicarboxylic acid which has similar structure to DPA has been investigated [32]. Solid-state material characterization techniques such as powder X-ray diffraction (PXRD), differential scanning calorimetry (DSC), fourier transform infrared (FTIR) spectroscopy, laser diffractometry (LD) analysis, polarized light microscopy (PLM) and scanning electron microscopy (SEM) were performed for PCA-DPA cocrystal characterization. Their solubility, dissolution rate, stability and tabletability studies were also investigated.
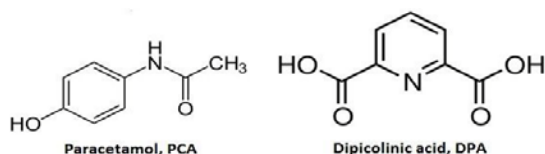

Fig. 1: Chemical structure of paracetamol (PCA) and Dipicolinic acid (DPA)

MATERIALS AND METHODS

Materials

Paracetamol was purchased from Zhejiang Kangle Pharmaceutical Co., Ltd. (Wenzhou, China). Dipicolinic acid (DPA) was obtained from Sigma-Aldrich, Co. (MO, USA). Methanol (ACS grade), potassium dihydrogen phosphate (KH_2PO4) and sodium hydroxide (NaOH) were obtained from Merck KGaA (Darmstadt, Germany). Acetonitrile (HPLC grade) was obtained from J. T. Baker, Inc. (NJ, USA). High purity of carbon dioxide (CO_2, purity of 99.95%) was purchased from PT Intergas (Jakarta, Indonesia). Polytetrafluoroethylene (PTFE) membrane with a size of 0.22 μm was purchased from Fioroni Filters (Ingre, France).

Experimental procedures

Cocrystallization by rapid evaporation process

Equimolar (1:1 mol ratio) quantities of PCA and DPA were dissolved in 20 ml of methanol and mixed under sonication at 40 °C for 10 min. The resulting solution was then placed into crystallizing disk and heated at 70 °C for 5 h using hot plate to evaporate the solvent. The dried solid was collected and placed in the glass vial for further analysis. The cocrystal product from this experiment was further namely as PCA-DPA-RE.

SAS cocrystallization apparatus

Cocrystallization was conducted using a custom-built supercritical anti-solvent (SAS) apparatus as shown in fig. 2. Solution reservoir (9) was a 110 ml Pyrex dropping funnel. High-pressure pump for CO_2 (3) was a Thar P-50 pump (Thar Technology, PA, USA). High-pressure pump for solution (8) was a Lab Alliance 1200 series (Lab Alliance, PA, USA). The precipitation chamber (7) was made of stainless steel 316 (SS316) with 100 ml internal volume and water jacket to control the temperature of precipitator. To observe the process of particle formation, a pair of glass windows was installed in front and back side of the precipitation chamber. A stainless steel capillary tube with internal diameter of 2.54×10^{-4} m was used as a nozzle and it was placed on the top of precipitation chamber. The CO_2 precooler (2) and preheater (6) were a shell and tube type. The inner tube was a coiled tube with 0.6 m length and 3.175×10^{-3} m outside diameter that made of SS316. The shell was made from SS316 with 0.11 in diameter and 0.25 m length. The products were filtered using 0.22 μm polytetrafluoroethylene (PTFE) membrane filter (10). Pressure of the precipitation chamber was controlled using a model 26-1721-24 back pressure regulator (11), manufactured by Tescom, Co. (MN, USA). The precooler and CO_2 pump temperature was maintained using cooling circulator (4).
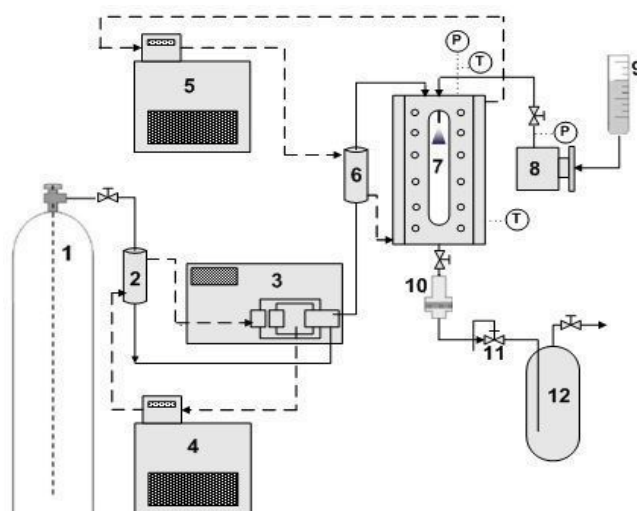

Fig. 2: Schematic diagram of custom-built SAS apparatus (1) CO_2 cylinder, (2) precooler, (3) high-pressure pump for CO_2, (4) cooling bath, (5) heating bath, (6) preheater, (7) precipitation chamber, (8) high-pressure pump for solution, (9) solution reservoir, (10) filter, (11) back pressure regulator, (12) separator

SAS Cocrystallization

Equimolar (1:1 mol ratio) quantities of PCA and DPA were dissolved in 20 ml of methanol and mixed under sonication at 40 °C for 10 min to obtain clear solution. The Cocrystallization started by supplying fresh CO_2 into precipitation chamber. After stable pressure (100 bar) and temperature (40 °C) were achieved, solution was sprayed into precipitation chamber at flow rate of 1 ml/min. At the same time, CO_2 was also pumped into the precipitation chamber at CO_2 flow rate of 30 g/min. After all solution was sprayed, CO_2 was supplied continuously for 30 min to remove all remaining solvent in the product inside the precipitation chamber and filter. Products were collected from the filter after depressurizing the precipitation chamber. The co crystal product from this experiment was further namely as PCA-DPA-SAS.

Characterization of cocrystal

Powder x-ray diffraction (PXRD)

Powder X-Ray Diffraction (PXRD) patterns were collected by a Rigaku Ultima IV X-ray diffractometer (Rigaku Co., Tokyo, Japan) using Cu Kα radiation (λ = 1.54 Å), a tube voltage of 40 kV and a tube current of 40 mA. Data were collected from 2 to 40 ° at continuous scan rate of 4 °/min.

Differential scanning calorimetry (DSC)

Thermal analysis of the samples was performed using DSC on a DSC Q20 (TA Instruments, DE, USA) which was calibrated for temperature and cell constants using indium. Samples (1-3 mg) crimped in aluminum pan were analyzed from 50 to 300 °C with heating rate of 10 °C/min. Samples were continuously purged with nitrogen at 50 ml/min.

Thermogravimetric analysis (TGA)

Thermogravimetric Analysis (TGA) was performed on a TGA Q50 (TA Instruments, DE, USA) instrument. Approximately 1-5 mg sample was heated from 50 to 300 °C in open aluminium pan at rate of 10 °C/min under nitrogen purge at flow rate of 50 ml/min.

Polarized light microscopy (PLM)

All Polarized Light Microscopy (PLM) experiments were performed using BX-50 polarizing microscope (Olympus, Tokyo, Japan). Photomicrographs were captured using Olympus SC-30 digital color camera and analyzed using Analysis getIT software.

Fourier transform infrared (FTIR) spectroscopy

IR spectra of the compounds were recorded on a FT/IR-6100 type A infrared spectrometer (JASCO, MD, USA) in ATR mode from 4000-700 cm^{-1} with a resolution of 4 cm^{-1}.

Particle size analysis

Particle size was determined by laser diffractometer (Mastersizer 2000, Malvern Instruments, USA) using the dry powder dispersing system Scirocco 2000 at pressure of 2 bar. Particle size was characterized by volume-weighted mean diameter D [4,3]. The particle size results represent average values over three measurements performed on each sample.

Scanning electron microscopy (SEM)

The morphology of the samples was analyzed using a JEOL JSM-6510 scanning electron microscopy (SEM, JEOL Ltd. Tokyo, Japan). Samples were mounted on a double-faced adhesive tape, sputtered with platinum. Scanning electron photographs were taken at an accelerating voltage of 5 kV.

High performance liquid chromatography (HPLC)

The concentrations of PCA in solutions was determined using High Performance Liquid Chromatography (HPLC) by Waters Alliance HPLC system which includes a Waters e2695 separation module, a Waters 2489 UV detector and a 4.6 mm×250 mm Sun Fire C18 with 5 μm column (Waters Corporation, Milford, MA). The mobile phase consisted of methanol and water (65/35, %v/v), with a flow rate of

1.0 ml/min. PCA was detected at 243 nm. The injection volume was 20 μl. Data acquisition and analysis was performed using software Empower 2.0.

Evaluation of cocrystal

Flowability analysis

Flow properties of PCA and cocrystals were determined in terms of Carr's Index and Hausner ratio. Bulk and tapped densities were measured in order to calculate Carr's Index and Hausner ratio. Hausner ratio was calculated from ratio of tapped density to bulk density, whereas Carr's Index was calculated according to the following equation:

Carr's index = [(tapped density-bulk density)/tapped density] x100.

The measurement of bulk and tapped density was done triplicate.

Drug content analysis

Accurately weighed amount of cocrystal was dissolved in methanol. The solution was then filtered through 0.22 μm PTFE syringe filter (Whatman, USA). PCA content was determined using HPLC ($n = 3$).

Solubility measurement

Excess amounts (500 mg) of the samples were suspended in 20 ml of phosphate buffer pH 5.8 in screw-capped glass vials and the suspension was stirred using a magnetic stirrer at 25 °C. After 24 h, the suspension was filtered through a paper filter; solid filtrate was dried and used for further PXRD analysis. The resulting solution was filtered again through a 0.22 μm nylon syringe filter (Whatman, USA). The filtered aliquot was sufficiently diluted. A concentration of PCA in solution was determined using HPLC.

In vitro dissolution study

To minimize the size effect on dissolution results, PCA and PCA-DPA-RE were sieved through 60-mesh sieves (mesh size 250 μm). Dissolution rate studies of the PCA, PCA-DPA-RE and PCA-DPA-SAS were performed in DT-700 dissolution apparatus (Erweka, Germany) according to the USP paddle method [33]. The experiment was conducted in 900 ml phosphate buffer solution pH 5.8. The temperature of the dissolution medium was kept at 37 °C and speed of the agitator was at 50 rpm. A specific amount of samples (equivalent to 500 mg of PCA) was added into the dissolution medium. At specific time intervals, 5 ml solution was withdrawn and concentration of PCA was determined using HPLC.

Stability study

Stability study was done by placing accurately weighed samples (approximately 100 mg) in 10 ml capped (closed condition) and uncapped glass vials (open condition). Both glass vials were placed into a stability chamber (Type KBF 720, Binder, Germany) at 40 °C/75% RH for one month, then the samples were analyzed by PXRD.

Powder compaction study

Evaluation of cocrystal was also performed by powder compaction analysis. In order to minimize the size difference between PCA and PCA-DPA-RE, both samples were sieved through 60-mesh sieves (mesh size 250 μm). Approximately 500 mg of powder was manually filled into a tableting die and compressed at pressures of 4.9-29.4 kN using hydraulic press apparatus (Perkin Elmer, MA, USA). Tablets (13 mm diameter) were allowed to relax overnight before their diameter, thickness and hardness were measured. The diameter and thickness of tablets were measured using a thickness gauge (Mitutoyo, Japan) and the tablet hardness was tested using a hardness tester (Type PTB 111, Pharma Test, Germany). Maximum breaking force, tablet diameter and tablet thickness were used to calculate tensile strength according to Eq. 1.

$$\sigma = \frac{2F}{\pi.D.T} \quad \text{...... (1)}$$

Where σ is tensile strength (MPa), F is the breaking force (N), D is the tablet diameter (mm) and T is the thickness of tablet (mm).

Tabletability profiles were obtained by plotting tensile strength as a function of compaction pressure.

RESULTS AND DISCUSSION

Powder x-ray diffraction (PXRD) analysis

PXRD is a useful method for identification of new crystalline phase from Cocrystallization experiments. Fig. 3d-e shows the PXRD patterns for the products from Cocrystallization process via rapid solvent evaporation and SAS Cocrystallization. The products obtained from each method have identical spectra. This result confirms that PCA-DPA cocrystal is successfully produced from SAS Cocrystallization experiment and it has similar internal crystal structure to PCA-DPA cocrystal from rapid solvent evaporation process. The diffractogram of PCA-DPA cocrystal was distinguishable from the individual compounds. It exhibited peaks at 2θ values of 8.58 °, 9.46 °, 10.50 °, 12.56 °, 13.60 °, 17.24 °, 24.12 ° and 26.78 °. The different peaks in the PXRD pattern of cocrystal could imply the existence of interactions between PCA and DPA to form new cocrystalline phase. Fig. 3d-e also shows, although the diffraction peaks characteristics of PCA-DPA-RE and PCA-DPA-SAS cocrystal were observed at the same 2θ position, intensity of diffraction peaks were different at several 2θ positions. The difference of diffraction peaks intensity can be explained by preferred orientation. Preferred orientation is a condition in which the distribution of crystal orientation is nonrandom and a specific crystalline frame may tend to cluster to a greater or lesser degree about some particular orientation [34]. These results show that the crystallization condition may control the crystallinity of the product.
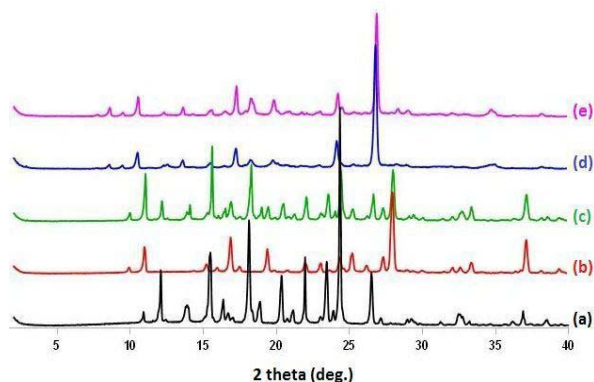

Fig. 3: Powder X-ray diffractograms of (a) PCA, (b) DPA, (c) physical mixture of PCA: DPA (1:1 mol ratio), (d) PCA-DPA-RE and (e) PCA-DPA-SAS

Thermal analysis

DSC and TGA experiments were carried out to study the thermal behavior of PCA-DPA cocrystal. The DSC thermograph for PCA, DPA, physical mixture of PCA and DPA in 1:1 mol ratio (PM), PCA-DPA-RE and PCA-DPA-SAS were given in fig. 4. It shows that PCA exhibited a melting endothermic peak at 170.23 °C, while DPA showed melting endothermic at 251.74 °C. DSC analysis for the physical mixture of PCA and DPA (1:1 mol ratio) showed two endothermic peaks (first endothermic peak at 164.82 °C, which could be attributed to the eutectic temperature of the mixture followed by second melting endotherm at 190.10 °C, which indicates the melting point of cocrystal). This observation was in accordance with the report from Lu *et al.*, 2008 [35], who demonstrated the use of DSC in cocrystal screening. They explained that formation of cocrystal could be predicted if there were two endothermic peaks (corresponding to eutectic mixture and cocrystal melting) obtained during the physical mixture melting process in DSC analysis [36-37]. DSC analysis of the products from cocrystallization experiments shows single endothermic peak which lies between the melting points of the parent compounds (PCA and DPA). PCA-DPA-RE and PCA-DPA-SAS exhibited endothermic melting point at 193.57 °C and 194.13 °C followed by broad endothermic peak corresponding to the decomposition of the cocrystals. This shift in the cocrystal's melting

point compared to the parent compounds might be due to the interaction (hydrogen bonding interaction) between API and coformer, resulted in different packing arrangement or change in the crystal lattice [38]. The single melting event of the cocrystals and no parent compound melting event in the thermograms of the cocrystals also indicate that there were no uncocrystallized parent compounds in the final product. A distinct cocrystal melting point in between the parent compound's melting point is in agreement with previous reports in the literature for a number of cocrystals. Schultheiss and Newman [8] conducted a survey on melting points of 50 reported cocrystalline samples and found that half of cocrystals had melting points between the pure components. The enthalpy of fusion (ΔH) of PCA-DPA-RE and PCA-DPA-SAS were 156.2 and 119.7 J/g, respectively. This result showed that cocrystal from SAS Cocrystallization process has lower enthalpy of fusion. This lower enthalpy of fusion in PCA-DPA cocrystal from SAS process might be due to the reduction of particle size after SAS process [18].
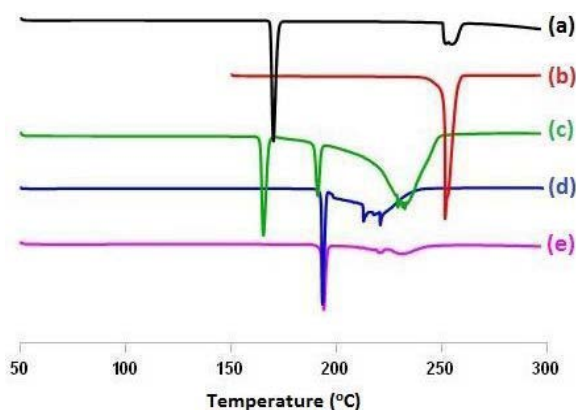

Fig. 4: DSC thermograms of (a) PCA, (b) DPA, (c) physical mixture of PCA: DPA (1:1 mol ratio), (d) PCA-DPA-RE and (e) PCA-DPA-SAS

TGA was conducted to analyze the changes in cocrystal weight in relation to the change of temperature (fig. 5). TGA curve showed no weight loss until melting suggesting that the PCA-DPA-RE and PCA-DPA-SAS cocrystals were not solvate or not hydrate. TGA of these cocrystals showed that there was mass loss after melting points, which attributed to the degradation of cocrystals.
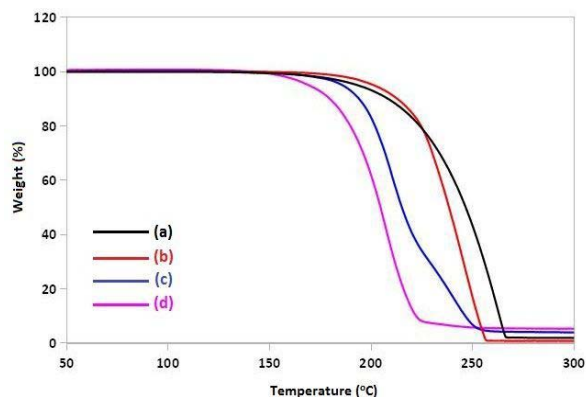

Fig. 5: TGA thermograms of (a) PCA, (b) DPA, (c) PCA-DPA-RE, and (d) PCA-DPA-SAS

Temperature-composition phase diagrams of PCA-DPA were constructed based on DSC experiments for binary mixtures of cocrystal formers at various molar compositions (fig. 6). This

diagram confirms that PCA-DPA cocrystal was an incongruent system [39], in which eutectic melting point occurred at ~164 °C and cocrystal melting point (peritectic point) occurred at ~190 °C.
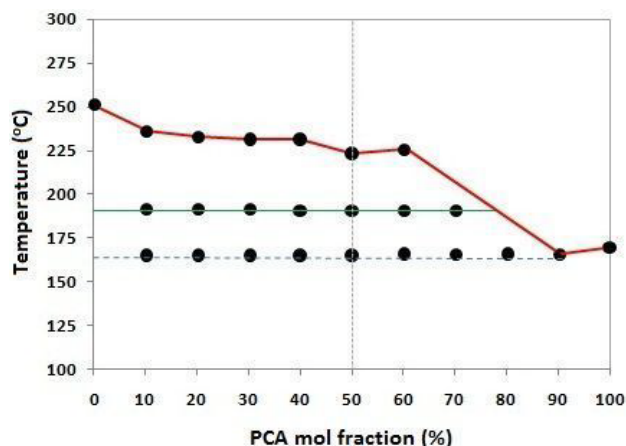

Fig. 6: Melting point phase diagram of PCA-DPA cocrystal system

Polarized light microscopy (PLM) images

The PLM photomicrographs of PCA, DPA and physical mixture of PCA and DPA (1:1 mol ratio) after recrystallized from methanol are shown in fig. 7a-c. The product from recrystallization of physical mixture of PCA and DPA (at 1:1 mol ratio) using methanol has a different crystal habit compared to its starting components. Thus it confirms the interaction between PCA and DPA to form new solid phase (cocrystal) which has different crystal habit. The crystal habit of a drug is an important variable in pharmaceutical manufacturing. The changes in the crystal habit of raw material after cocrystallization can influence its physicomechanical properties and it affects the performance of dosage form [40].

Fourier transform infrared (FTIR) spectroscopy analysis

FTIR spectroscopy can be used to confirm the formation of cocrystal. The changes in vibrational frequencies of the functional groups can be directly correlated with the changes in hydrogen bonding due to formation of cocrystal [41]. From the chemical structures of PCA and DPA (fig. 1), there are several functional groups which are able to form intermolecular hydrogen bonding, thus several possible synthon to form can be obtained. The FTIR spectra of PCA, DPA, PCA-DPA-RE and PCA-DPA-SAS cocrystal are shown in fig. 8. Table 1 shows the list of relevant IR bands for PCA, DPA and all cocrystals [42]. The results reveal the changes in the IR bands of the cocrystals compared to the pure components, indicating the presence of intermolecular hydrogen bonding.

The new bands at ~3300 cm^{-1} in the PCA-DPA cocrystal can be assigned to the intermolecular hydrogen bond interaction O···N-H between C=O (carbonyl functional group) in the DPA and N−H (amide functional group) in the PCA. The O−H stretch of DPA occurred at 3066.82 cm^{-1} for the pure coformer. The frequency of this stretch shifted into higher wavenumber (~3110-3200 cm^{-1}) in the PCA-DPA cocrystals prepared by each method. The transition of O−H stretch of DPA suggests that this group also participates in a hydrogen bond in the cocrystal product. Based on the changes in the frequency of these functional groups, we hypothesized the formation of cocrystal between PCA and DPA via heterosynthon formation between carboxylic acid (from DPA functional group) and amide groups (from PCA functional group) [43-44].

The FTIR analysis also can be used to determine whether proton transfer from carboxylic acid had occurred, which can differentiate the formed product between salt and cocrystal. In the formation of a salt species, there were typical carboxylate anions which have two carbonyl stretching bands: a strong asymmetrical band below 1600 cm^{-1} and a weaker symmetrical band near 1400 cm^{-1}. On the other hand, when the frequency of carbonyl group in carboxylic acid shifted to the higher energy (approximate frequency range of 1700-1730 cm^{-1}), a cocrystal species had formed [45]. Fig. 8c-d shows carbonyl functional group in PCA-DPA cocrystal shift into higher frequency of ~1720-1730 cm^{-1}. Therefore, proton transfer does not occur between PCA and DPA and thus confirms the cocrystal formation between PCA and DPA.
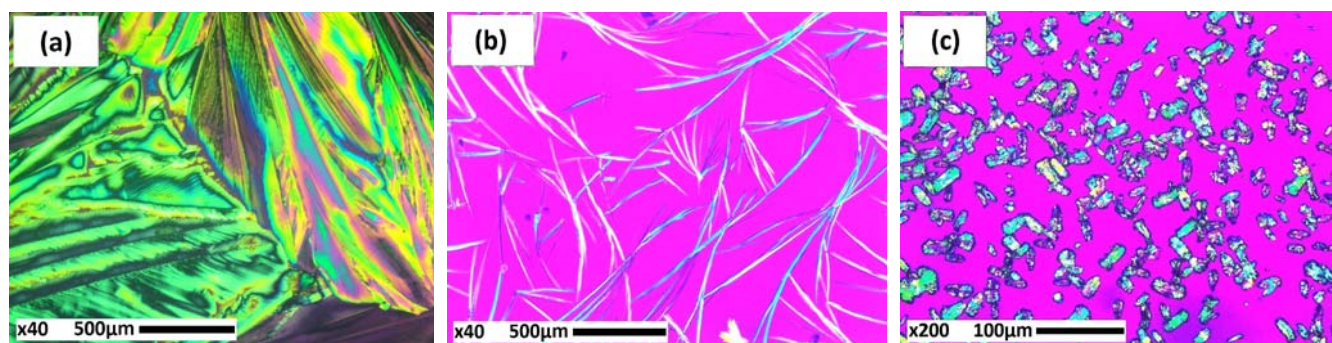

Fig. 7: Polarized light microscopy (PLM) images of (a) PCA, (b) DPA, (c) physical mixture of PCA: DPA (1:1 mol ratio) after recrystallized using methanol

Table 1: Bond stretching frequencies in PCA, DPA, PCA-DPA-RE and PCA-DPA-SAS, determined from FTIR analysis

Assignment	PCA	DPA	PCA-DPA-RE	PCA-DPA-SAS
ν(N−H)/cm^{-1}	3321.04	-	3346.69	3345.26
ν(O−H)/cm^{-1}	3158.38, 3107.24	3066.82	3231.15, 3162.63, 3116.98	3232.43, 3163.49, 3118.07
ν(C=O)/cm^{-1}	1650.21	1688.33	1723.62	1731.08
Intermolecular O···H−N(H-bond)/cm^{-1}	-	-	3300.69	3301.86

PCA: Paracetamol, DPA: Dipicolinic acid, RE: Rapid evaporation, SAS: Supercrtical antisolvent.
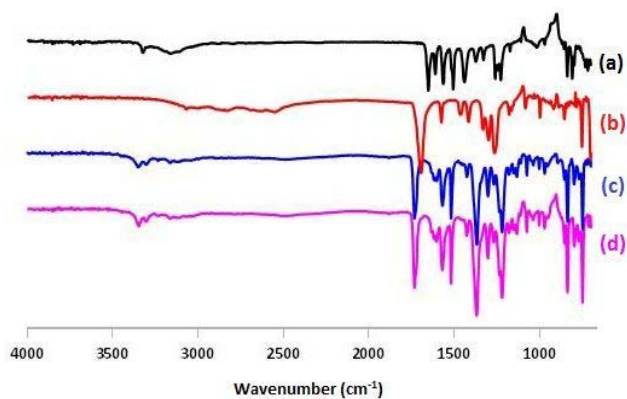
Fig. 8: FTIR spectra of (a) PCA, (b) DPA, (c) PCA-DPA-RE and (d) PCA-DPA-SAS

Flowability and particle size analysis

Flowability of PCA and resulted cocrystals are shown in table 2. The calculated Carr's index and Hausner ratio of PCA and cocrystals which represent flowability, showed that cocrystals have improved flowability compared to PCA. The improvement in flowability of PCA-DPA-RE could be due to the reduction of cohesiveness of the powder. Less irregular habit (fewer points for physical contact) of PCA-DPA-RE compared to PCA resulted in the reduction of interparticle contact areas and thus reducing cohesiveness of the powder, which can be confirmed by SEM picture. Similar observation was also found by another researcher [46]. Generally, particles with smaller size tend to be more cohesive and have poorer flowability compared to larger particle [38]. However, PCA-DPA-SAS, which has smaller particle size of 4.18±0.054 μm, has better flowability than PCA which has larger particle size of 45.33±0.439 μm. This could be attributed due to their more regular polyhedral crystal habit that improved the free flowing of the powder compared to PCA powder. PCA powder has larger size but it has a habit that led to higher contact area. On the other hand, slightly reduction in the flowability of PCA-DPA-SAS compared to that of PCA-DPA-RE (particle size of 64.93±0.095 μm) may be attributed to their smaller particle size. These findings show that the flowability of PCA-DPA

cocrystal was preferably improved compared to pure PCA. Fig. 9 shows that SAS process can produce PCA-DPA cocrystal with smaller average particle size and particle size distribution (fig. 9d). This result shows that SAS process was an efficient process to produce submicron size of PCA-DPA cocrystal.
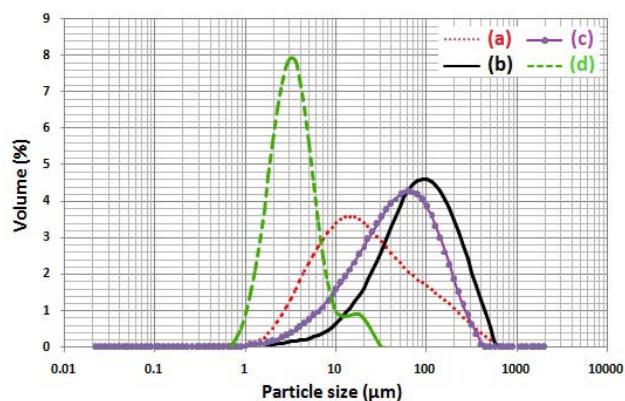

Fig. 9: Particle size distribution (PSD) profile of (a) PCA, (b) DPA, (c) PCA-DPA-RE and (d) PCA-DPA-SAS

Scanning electron microscopy (SEM) analysis

Morphology of the API has influenced various pharmaceutical parameters such as flowability, compaction, compressibility, solubility and dissolution characteristics of drug powder [16]. Fig. 10 shows SEM micrographs of PCA, DPA and PCA-DPA cocrystals. PCA crystals exhibited an irregular rod-like or columnar habit (fig. 10a). This is in accordance to previous report [46]. DPA crystal showed thin plate-like crystals (fig. 10b). Fig. 10c-d shows SEM micrographs of PCA-DPA-RE and PCA-DPA-SAS. PCA-DPA-RE cocrystal showed irregular rod-like crystals, whereas PCA-DPA-SAS cocrystal showed a different crystal habit. It showed a prismatic polyhedral crystals and smaller particle size compared to PCA-DPA-RE. Differences in crystal habit obtained due to differences in the environmental conditions of crystal growth, which lead to the formation of crystals with different external shapes (crystal habit) but it has the same internal structure [47].
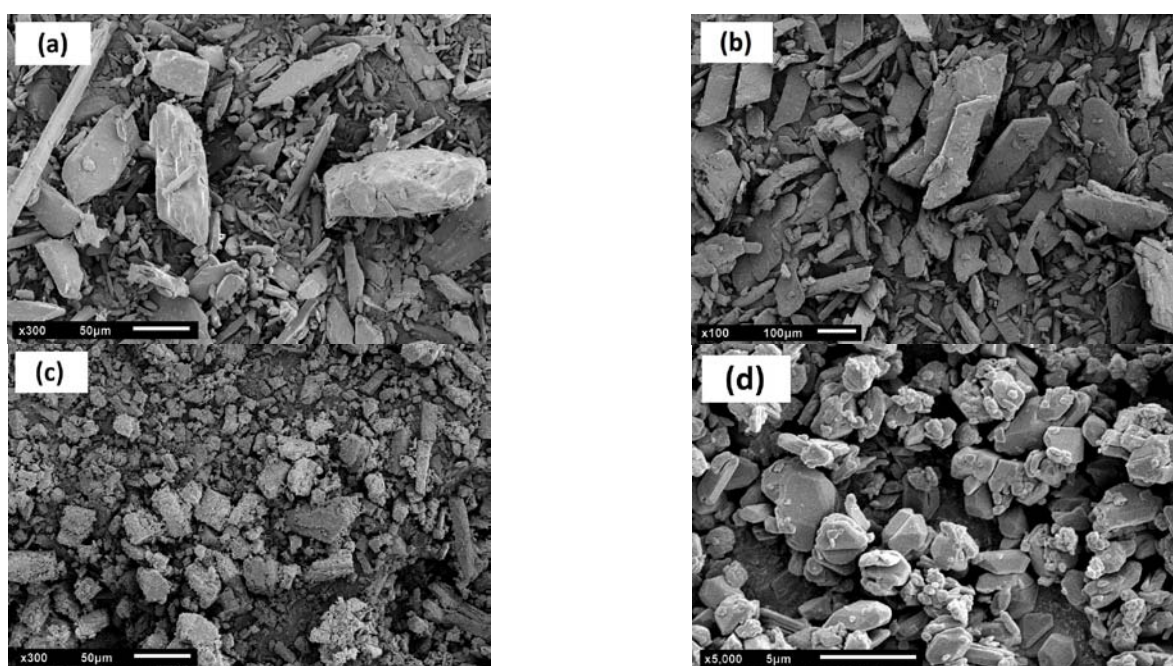

Fig. 10: SEM images of (a) PCA, (b) DPA, (c) PCA-DPA-RE and (d) PCA-DPA-SAS

Table 2: Flow properties of PCA, PCA-DPA-RE and PCA-DPA-SAS

Sample	Carr's index (%)	Hausner Ratio	Flow characteristic
PCA	43.18±1.31	1.76±0.04	Very, very poor
PCA-DPA-RE	22.27±1.17	1.29±0.02	Passable
PCA-DPA-SAS	27.21±1.09	1.37±0.02	Poor

PCA: Paracetamol, DPA: Dipicolinic acid, RE: Rapid evaporation, SAS: Supercrtical antisolvent

Drug content analysis

PCA content in PCA-DPA cocrystal was determined by HPLC. The percentage of PCA content in PCA-DPA-RE and PCA-DPA-SAS were 44.98±0.77 and 41.83±0.66 (%), respectively. The calculated content of DPA was 53.91±2.991 and 58.17±0.66 (%) for PCA-DPA-RE and PCA-DPA-SAS. The molar ratio of PCA and DPA was determined to be 1:1 since the theoretical percentage of the two components are 47.49% and 52.51%. The low PCA content in PCA-DPA-SAS might be due to the slight solubility of PCA in sCO_2 during the process, which was confirmed by other researchers [48].

Powder compaction analysis

Fig. 11 shows the compaction pressure-tablet tensile strength profiles for PCA, DPA, PCA-DPA-RE and PCA-DPA-SAS cocrystal. Tabletability profile was determined over a compaction pressure range of 4.9 kN to 29.4 kN. The tablet tensile strength of PCA could not be measured at all compression pressures because the tablets capped immediately after being taken out from the die. Similar finding was also found by another researcher [49]. In contrast, DPA, PCA-DPA-RE and PCA-DPA-SAS exhibited much better tabletability as shown in fig. 11b-d. Tablet tensile strength has to reach 2 MPa to ensure the integrity of a pharmaceutical tablet [50]. This criteria was fulfilled by PCA-DPA-RE at >14.7 kN compaction pressure and >29.4 kN compaction pressure for PCA-DPA-SAS. This result indicates better tabletability of PCA-DPA-RE compared to PCA-DPA-SAS. Generally for most powdered pharmaceuticals, compaction of smaller particles resulted stronger tablets because smaller particles provide larger total area for bonding than larger particles [51]. Due to the fact that PCA-DPA-SAS process had smaller particle size than PCA-DPA-RE, the tensile strength of tablets produced from PCA-DPA-SAS should be higher than the tablet tensile strength of PCA-DPA-RE. However, the tablets of PCA-DPA-SAS showed lower mechanical strength compared to the tablets of PCA-DPA-RE. It has been reported that poor compressibility of drug crystals can be attributed to the presence of crystal faces that give poor adhesion to other crystals and the absence of the faces that are required for optimal adhesion [52].
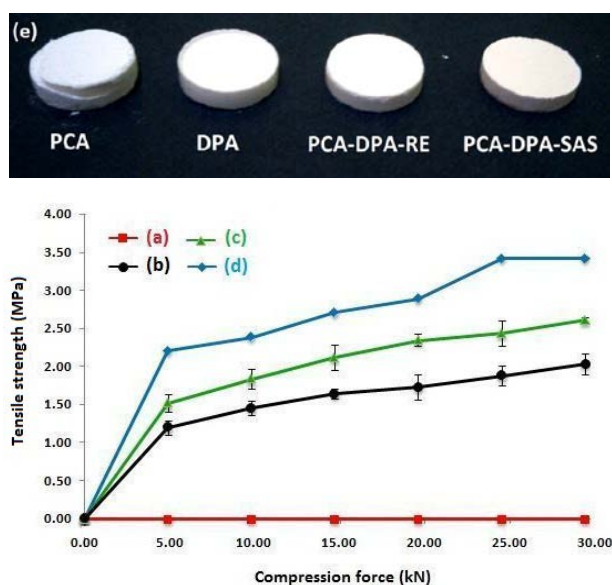

Fig. 11: Tablet ability of (a) PCA, (b) PCA-DPA-SAS, (c) PCA-DPA-RE, (d) DPA, and (e) overview of each tablet

Here in this study,, for the more regular habit (polyhedral habit) of PCA-DPA-SAS led to lower contact area compared to irregular rod-like crystal habit of PCA-DPA-RE. This can affect the inter-particulate bonding between these crystals, and resulting in different compression properties [53]. Better compression was observed for PCA-DPA-RE which has more irregular size (larger PSD) and habit (shape). In this case, uniform-sized PCA-DPA-SAS cocrystal might be difficult to orient in different direction, resulting in poor compaction. In contrast, PCA-DPA-RE cocrystal has different size and more irregular habit. Fines from this product could fill into cavities in between larger particles [54]. This resulted in better compaction behavior of PCA-DPA-RE compared to PCA-DPA-SAS. Differences in tableting properties of PCA-DPA-RE and PCA-DPA-SAS may also be attributed to the difference in their flow properties. Because of the better flowability of PCA-DPA-RE, the powder filled homogeneously into the die and the contact between crystals was more intensive. Therefore, the input of energy into the powder is much more effective, resulted in increased tensile strength of the tablet [55].

Dissolution test

To verify whether formation of cocrystals could modify the dissolution behavior of PCA, the release of PCA from PCA-DPA-RE and PCA-DPA-SAS cocrystal was investigated via dissolution experiments and compared to PCA. The dissolution profiles of PCA, PCA-DPA-RE and PCA-DPA-SAS cocrystals are shown in fig. 12. It is shown that both PCA-DPA cocrystals exhibited improvement in dissolution rate compared to pure PCA. The improvement in dissolution of PCA-DPA-RE cocrystal compared to PCA might be due to reduction of powder cohesiveness. On the other side, improvement in dissolution of PCA-DPA-SAS co crystal compared to PCA is likely due to the significant reduction of particle size. Weibull equation and similarity factor were used to compare the dissolution profile between PCA and PCA-DPA cocrystal [18, 56]. The dissolution rate coefficient (kw) value obtained from Weibull equation of the PCA, PCA-DPA-RE and PCA-DPA-SAS were 0.118 min^{-1}, 0.202 min^{-1} and 0.289 min^{-1}. Based on this result, the dissolution rate of PCA-DPA-RE was enhanced approximately 1.72 times compared to PCA and the dissolution rate of PCA-DPA-SAS was enhanced approximately 2.45 times compared to PCA. Furthermore, the different factor (*f1*) and similarity factor (*f2*) were used to analyze the dissolution profile.

$$f1 = \frac{\sum_{j=1}^{n} |Rj - Tj|}{\sum_{j=1}^{n} Rj} \, x \, 100$$

............(2)

$$f2 = 50 \, x \, log\left\{ \left[1 + \frac{1}{n} \sum_{j=1}^{n} |Rj - Tj|^\wedge 2 \right]^{-0.5} x \, 100 \right\}$$

............(3)

Where *Rj* and *Tj* are the cumulative percentage dissolved at each of selected *n* time points of the unprocessed particles (reference) and processed particles (test product), respectively. In general, the dissolution profiles were taken as similar with *f1* value lower than 15 and *f2* value higher than 50. The comparison of dissolution profile using *f2* has also been adopted by food and drug administration (FDA) and european medicines agency (EMEA) in the assessment of similarity between two dissolution profiles [18,56]. In this study, comparison between dissolution profile of PCA and PCA-DPA-RE resulted in similarity for their dissolution profiles as

indicated by the difference and similarity factor (*f1* and *f2*) value of 11.06 and 53.51, respectively. On the other hand, comparison between dissolution profile of PCA and PCA-DPA-SAS resulted in difference for their dissolution profile as indicated by the difference and similarity factor (*f1* and *f2*) value of 15.31 and 46.11, respectively. This result confirmed that the dissolution character of PCA-DPA-SAS cocrystal was improved and exhibited different profile to PCA.
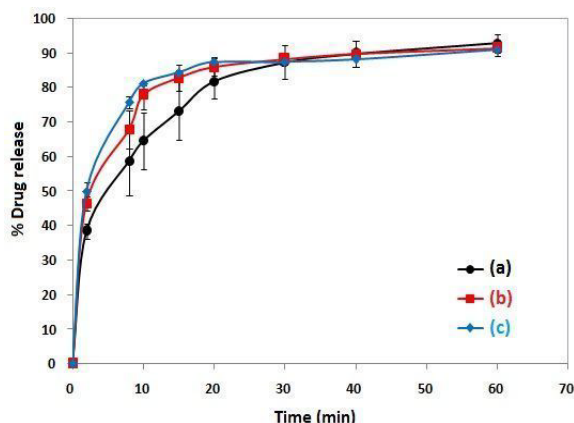

Fig. 12: Dissolution profile of (a) PCA, (b) PCA-DPA-RE and (c) PCA-DPA-SAS

Solubility analysis

The solubility of PCA and PCA-DPA co crystal was determined at 24 h in phosphate buffer pH 5.8. The results of solubility study show that the solubility values of PCA-DPA-RE and PCA-DPA-SAS cocrystals were 6297.5 ppm and 6277.5 ppm, respectively. Although this is lower than the solubility of PCA (14989.6 ppm), it does not cause any problem in the dissolution of this compound because more than 80% PCA has already been released (dissolved) in the dissolution medium in 30 min as required for its dissolution requirement [33]. The incorporation of less soluble conformer into the crystal lattice of cocrystals may reduce the solubility of PCA, as the aqueous solubility (25 °C) of DPA (5 mg/ml) is less than that of PCA (12.78 mg/ml). The effective arrangement of crystal packing in cocrystals via supra molecular interactions, such as hydrogen bonding, will also contribute to their reduced solubility. The solid residues obtained after the solubility studies were then characterized by PXRD. The PXRD patterns of PCA and PCA-DPA co crystal after solubility study (fig. 13) were found to be similar to that of their original forms indicating stability of these cocrystals in the solubility medium for 24 h.
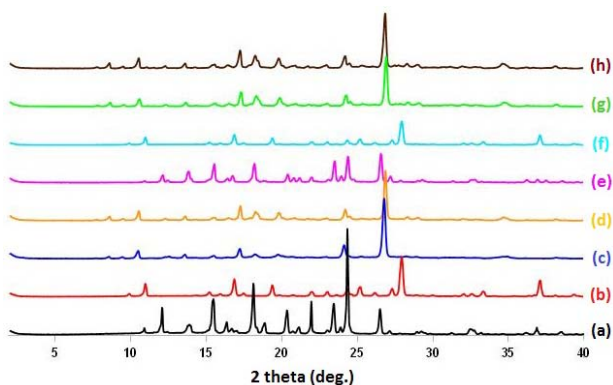

Fig. 13: Powder X-ray diffractograms before solubility study for (a) PCA, (b) DPA, (c) PCA-DPA-RE, (d) PCA-DPA-SAS and after solubility study in phosphate buffer pH 5.8 for (e) PCA, (f) DPA, (g) PCA-DPA-RE, (h) PCA-DPA-SAS

Stability study

PCA, PCA-DPA-RE and PCA-DPA-SAS cocrystals were kept under accelerated stability conditions of 40 °C/75% RH and analyzed by PXRD after 1 mo. The results of PXRD analysis demonstrate that the PXRD patterns of PCA, PCA-DPA-RE and PCA-DPA-SAS cocrystal did not change (fig. 14). This analysis indicates that PCA-DPA-RE and PCA-DPA-SAS cocrystal were physically stable under accelerated stability condition studied.
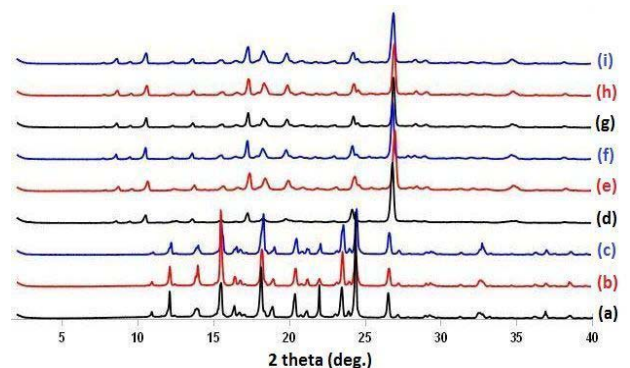

Fig. 14: Powder X-ray diffractograms resulting from stability study under accelerated conditions (a) PCA day 0, (b) PCA day 30 in open condition, (c) PCA day 30 in close condition, (d) PCA-DPA-RE day 0, (e) PCA-DPA-RE day 30 in open condition, (f) PCA DPA-RE day 30 in close condition, (g) PCA-DPA-SAS day 0, (h) PCA-DPA-SAS day 30 in open condition, and (i) PCA-DPA-SAS day 30 in close condition

CONCLUSION

In this study, we show successful production of PCA and DPA cocrystal using SAS Cocrystallization and traditional rapid solvent evaporation process. The formation of new crystalline phases was confirmed from PXRD, DSC, FTIR, PLM and SEM analysis. The particle size of cocrystal particles produced by SAS was smaller than those produced by traditional rapid solvent evaporation process. Dissolution test of PCA-DPA cocrystal from SAS process shows significant enhancement in dissolution rate approximately 2.45 times compared to PCA alone. The cocrystals were found to be stable over the period of 1 mo confirmed from stability studies. PCA-DPA cocrystals from SAS process and traditional rapid solvent evaporation process show remarkable enhancement in the tableting properties compared to PCA. This study demonstrates the ability of SAS process to produce submicron size of PCA-DPA cocrystal with altered physicochemical properties in a single step process.

ABBREVIATION

API-Active Pharmaceutical Ingredient, CO_2-Carbon dioxide, DELOS-Depressurization of an Expanded Liquid Organic Solvent, DPA-Dipicolinic acid, DSC-Differential Scanning Calorimetry, EMEA-European Medicines Agency, FDA-Food and Drug Administration, FTIR-Fourier Transform Infrared Spectroscopy, GAS-Gas Anti-solvent, HPLC-High Performance Liquid Chromatography, HSPM-Hot Stage Polarized Microscopy, IR-Infrared, KH_2PO4-Potassium dihydrogen phosphate, LD-Laser diffraction, NaOH-Sodium hydroxide, PCA-Paracetamol, PGSS-Particles from Gas Saturated Solutions, PLM-Polarized Light Microscopy, PM-Physical Mixture, PTFE-Polytetrafluoroethylene, PXRD-Powder X-ray Diffraction, RESS-Rapid Expansion of Supercritical Solutions, RH-Relative Humidity, SAA-Supercritical Assisted Atomization, SAS-Supercritical Anti solvent, SCF-Supercritical Fluid, sCO_2-Supercritical Carbon Dioxide, SEA-Supercritical Enhanced Atomization, SEDS-Solution

Enhanced Dispersion by Supercritical fluids, SEM-Scanning Electron Microscope, TGA-Thermogravimetric Analysis.

CONFLICT OF INTERESTS

The authors declared no conflicts of interest with respect to the authorship and/or publication.

REFERENCES

1. Martin FA, Pop MM, Borodi G, Filip X, Kacso I. Ketoconazole salt and co-crystals with enhanced aqueous solubility. Cryst Growth Des 2013;13:4295-304.
2. Gao Y, Gao J, Liu Z, Kan H, Zu H, Sun W, *et al.* Coformer selection based on degradation pathway of drugs: a case study of adefovir dipivoxil-saccharin and adefovir dipivoxil-nicotinamide cocrystals. Int J Pharm 2012;438:327-35.
3. Wang ZZ, Chen JM, Lu TB. Enhancing the hygroscopic stability of S-Oxiracetam via pharmaceutical cocrystal. Cryst Growth Des 2012;12:4562-6.
4. Sanphui P, Kumar SS, Nangia A. Pharmaceutical cocrystals of niclosamide. Cryst Growth Des 2012;12:4588-99.
5. Karki S, Friscic T, Fabian L, Laity PR, Day GM, Jones W. Improving mechanical properties of crystalline solids by cocrystal formation: new compressible forms of paracetamol. Adv Mater 2009;21:3905-9.
6. Cheney ML, Shan N, Healey ER, Hanna M, Wojtas L, Zaworotko MJ, *et al.* Effects of crystal form on solubility and pharmacokinetics: a crystal engineering case study of lamotrigine. Cryst Growth Des 2010;10:394-405.
7. Trask AV. An overview of pharmaceutical cocrystals as intellectual property. Mol Pharm 2007;4:301-9.
8. Schultheiss N, Newman A. Pharmaceutical cocrystals and their physicochemical properties. Cryst Growth Des 2009;9:2950-67.
9. Trask AV, Jones W. Crystal engineering of organic cocrystals by the solid-state grinding approach. Top Curr Chem 2005;254:41-70.
10. Lin HL, Wu TK, Lin SY. Screening and characterization of cocrystal formation of metaxalone with short-chain dicarboxylic acids induced by solvent-assisted grinding approach. Thermochim Acta 2014;575:313-21.
11. Fucke K, Myz SA, Shakhtshneider TP, Boldyreva EV, Griesser UJ. How good are the crystallisation methods for co-crystals? A comparative study of piroxicam. New J Chem 2012;36:1969-77.
12. Takata N, Shiraki K, Takano R, Hayashi Y, Terada K. Cocrystal screening of stanolone and mestanolone using slurry crystalization. Cryst Growth Des 2008;8:3032-7.
13. Chen JM, Wang ZZ, Wu CB, Li S, Lu TB. Crystal engineering approach to improve the solubility of mebendazole. CrystEngComm 2012;14:6221-9.
14. Berry DJ, Seaton CC, Clegg W, Harrington RW, Coles SJ, Horton PN, *et al.* Applying hot-stage microscopy to co-crystal screening: a study of nicotinamide with seven active pharmaceutical ingredients. Cryst Growth Des 2008;8:1697-712.
15. Yamashita H, Hirakura Y, Yuda M, Teramura T, Terada K. Detection of cocrystal formation based on binary phase diagrams using thermal analysis. Pharm Res 2013;30:70-80.
16. Moradiya H, Islam MT, Woollam GR, Slipper IJ, Halsey S, Snowden MJ, *et al.* Continuous cocrystallization for dissolution rate optimization of a poorly water soluble drug. Cryst Growth Des 2014;14:189-98.
17. Alhalaweh A, Velaga SP. Formation of cocrystals from stoichiometric solutions of incongruently saturating systems by spray drying. Cryst Growth Des 2010;10:3302-5.
18. Hiendrawan S, Veriansyah B, Tjandrawinata RR. Micronization of fenofibrate by rapid expansion of supercritical solution. J Ind Eng Chem 2014;20:54-60.
19. Vieira de Melo SAB, Danh LT, Mammucari R, Foster NR. Dense CO2 antisolvent precipitation of levothyroxine sodium: a comparative study of GAS and ARISE techniques based on morphology and particle size distributions. J Supercrit Fluids 2014;93:112-20.
20. Padrela L, Rodrigues MA, Velaga SP, Matos HA, de Azevedo EG. Formation of indomethacin-saccharin cocrystals using supercritical fluids technology. Eur J Pharm Sci 2009;38:9-17.
21. Padrela L, Rodrigues MA, Velaga SP, Fernandes AC, Matos HA, de Azevedo EG. Screening for pharmaceutical cocrystals using the supercritical fluid enhanced atomization process. J Supercrit Fluids 2010;53:156-64.
22. Padrela L, Rodrigues MA, Tiago J, Velaga SP, Matos HA, de Azevedo EG. Tuning physicochemical properties of theophylline by cocrystallization using the supercritical fluid enhanced atomization technique. J Supercrit Fluids 2014;86:129-36.
23. Ober CA, Gupta RB. Formation of itraconazole-succinic acid cocrystals by gas antisolvent cocrystallization. AAPS PharmSciTech 2012;13:1396-406.
24. Ober CA, Montgomery SE, Gupta RB. Formation of itraconazole/l-malic acid cocrystals by gas antisolvent cocrystallization. Powder Technol 2013;236:122-31.
25. Neurohr C, Revelli AL, Billot P, Marchivie M, Lecomte S, Laugier S, *et al.* Naproxen-nicotinamide cocrystals produced by CO2 antisolvent. J Supercrit Fluids 2013;83:78-85.
26. Mullers KC, Paisana M, Wahl MA. Simultaneous formation and micronization of pharmaceutical cocrystals by rapid expansion of supercritical solutions (RESS). Pharm Res 2015;32:702-13.
27. Rossmann M, Braeuer A, Leipertz A, Schluecker E. Manipulating the size, the morphology and the polymorphism of acetaminophen using supercritical antisolvent (SAS) precipitation. J Supercrit Fluids 2013;82:230-7.
28. Li G, Chu J, Song ES, Row KH, Lee KH, Lee YW. Crystallization of acetaminophen micro-particle using supercritical carbon dioxide. Korean J Chem Eng 2006;23:482-7.
29. Tabernero A, del Valle EMM, Galan MA. Precipitation of tretinoin and acetaminophen with solution enhanced dispersion by supercritical fluids (SEDS). Powder Technol 2012;217:177-88.
30. Srirambhatla VK, Kraft A, Watt S, Powell AV. Crystal design approaches for the synthesis of paracetamol co-crystals. Cryst Growth Des 2012;12:4870-9.
31. Andre V, Fatima M, da Piedad M, Duarte MT. Revisiting paracetamol in a quest for new co-crystals. CrystEngComm 2012;14:5005-14.
32. Sander JRG, Bucar DK, Henry RF, Baltrusaitis J, Zhang GGZ, Macgillivray LR. A red zwitterionic co-crystal of acetaminophen and 2,4-pyridinecarboxylic acid. J Pharm Sci 2010;99:3676-83.
33. United States Pharmacopeial Convention, Inc., The United States Pharmacopeia. 31st ed. Rockville: United States Pharmacopeial Convention, Inc; 2008.
34. Kim MS, Lee S, Park JS, Woo JS, Hwang SJ. Micronization of cilostazol using supercritical antisolvent (SAS) process: effect of process parameters. Powder Technol 2007;177:64-70.
35. Lu E, Hornedo NR, Suryanarayanan R. A rapid thermal method for cocrystal screening. CrystEngComm 2008;10:665-8.
36. Dhumal RS, Kelly AL, York P, Coates PD, Paradkar A. Cocrystallization and simultaneous agglomeration using hot melt extrusion. Pharm Res 2010;27:2725-33.
37. Manin AN, Voronin AP, Drozd KV, Manin NG, Brandl AB, Perlovich GL. Cocrystal screening of hydroxybenzamides with benzoic acid derivatives: a comparative study of thermal and solution-based methods. Eur J Pharm Sci 2014;65:56-64.
38. Mulye SP, Jamadar SA, Karekar PS, Pore YV, Dhawale SC. Improvement in physicochemical properties of ezetimibe using a crystal engineering technique. Powder Technol 2012;222:131-8.
39. Manin AN, Voronin AP, Manin NG, Vener MV, Shishkina AV, Lermontov AS. Salicylamide cocrystals: screening, crystal structure, sublimation thermodynamics, dissolution, and solid-state DFT calculations. J Phys Chem B 2014;118:6803-14.
40. Garekani HA, Ford JL, Rubinstein MH, Siahboomi ARR. Formation and compression characteristics of prismatic polyhedral and thin plate-like crystals of paracetamol. Int J Pharm 1999;187:77-89.
41. Chadha R, Saini A, Jain DS, Venugopalan P. Preparation and solid-state characterization of three novel multicomponent solid forms of oxcarbazepine: improvement in solubility through saccharin cocrystal. Cryst Growth Des 2012;12:4211-24.
42. Moynihan HA, Hare IPO. Spectroscopic characterisation of the monoclinic and orthorhombic forms of paracetamol. Int J Pharm 2002;247:179-85.

43. Wang L, Tan B, Zhang H, Deng Z. Pharmaceutical cocrystals of diflunisal with nicotinamide or isonicotinamide. Org Process Res Dev 2013;17:1413-8.
44. Chow SF, Chen M, Shi L, Chow AHL, Sun CC. Simultaneously improving the mechanical properties, dissolution performance, and hygroscopicity of ibuprofen and flurbiprofen by cocrystallization with nicotinamide. Pharm Res 2012;29:1854-65.
45. Brittain HG. Vibrational spectroscopic studies of cocrystals and salts.3. cocrystal products formed by benzenecarboxylic acids and their sodium salts. Cryst Growth Des 2010;10:1990-2003.
46. Kaialy W, Larhrib H, Chikwanha B, Shojaee S, Nokhodchi A. An approach to engineer paracetamol crystals by antisolvent crystallization technique in presence of various additives for direct compression. Int J Pharm 2014;464:53-64.
47. Renuka, Singh SK, Gulati M, Kaur I. Characterization of solid state forms of glipizide. Powder Technol 2014;264:365-76.
48. Rossmann M, Braeuer A, Dowy S, Gallinger TG, Leipertz A, Schluecker E. Solute solubility as criterion for the appearance of amorphous particle precipitation or crystallization in the supercritical antisolvent (SAS) process. J Supercrit Fluids 2012;66:350-8.
49. Perumalla SR, Shi L, Sun CC. Ionized form of acetaminophen with improved compaction properties. Cryst Eng Comm 2012;14:2389-90.
50. Chattoraj S, Shi L, Chen M, Alhalaweh A, Velaga S, Sun CC. Origin of deteriorated crystal plasticity and compaction properties of a 1:1 cocrystal between piroxicam and saccharin. Cryst Growth Des 2014;14:3864-74.
51. Sun C, Grant DJW. Effects of initial particle size on the tableting properties of L-lysine monohydrochloride dihydrate powder. Int J Pharm 2001;251:221-8.
52. Garekani HA, Sadeghi F, Badiee A, Mostafa SA, Siahboomi ARR. Crystal habit modifications of ibuprofen and their physicomechanical characteristics. Drug Dev Ind Pharm 2001;27:803-9.
53. Nokhodchi A, Bolourtchian N, Dinarvand R. Crystal modification of phenytoin using different solvents and crystallization conditions. Int J Pharm 2003;250:85-97.
54. Aher S, Dhumal R, Mahadik K, Ketolainen J, Paradkar A. Effect of cocrystallization techniques on compressional properties of caffeine/oxalic acid 2:1 cocrystal. Pharm Dev Technol 2013;18:55-60.
55. Rasenack N, Muller BW. Crystal habit and tableting behavior. Int J Pharm 2002;244:45-57.
56. Hiendrawan S, Veriansyah B, Tjandrawinata RR. A bottom-up process approach for micronization of ibuprofen. J Chem Pharm Res 2015;7:708-15.